Liquid Phase – Pulsed Laser Ablation: A route to fabricate different carbon nanostructures

Ahmed Al-Hamaoy[a,f,g], Evans Chikarakara[a], Hussein Jawad[f], Kapil Gupta[b], Dinesh Kumar[b], M.S. Ramachandra Rao[b], Satheesh Krishnamurthy[c], Muhammad Morshed[a], Eoin Fox[d], Dermot Brougham[d], Xiaoyun He[a,e], Mercedes Vázquez[a,e], Dermot Brabazon[a,e],*

[a] Advanced Processing Technology Research Centre, Dublin City University, Dublin 9,
[b] IrelandbDepartment of Physics, Nano Functional Materials Technology Centre and Materials Science Research Centre, Indian Institute of Technology (IIT) Madras,Chennai 600 036, India,
[c] Materials Engineering, The Open University, Milton Keynes, MK7 6AA, United Kingdom,
[d] School of Chemical Sciences, Dublin City University, Dublin 9, Ireland,
[e] Irish Separation Science Cluster (ISSC) National Centre for Sensor Research, Dublin City University, Dublin 9, Ireland,
[f] Institute of Laser for Postgraduate Studies, University of Baghdad, Iraq
[g] Mechanical Engineering Department, College of Engineering, University of Anbar, Iraq

ABSTRACT

Carbon nanostructures in various forms and sizes, and with different speciation properties have been prepared from graphite by Liquid Phase – Pulsed Laser Ablation (LP-PLA) using a high frequency Nd:YAG laser. High energy densities and pulse repetition frequencies of up to 10 kHz were used in this ablation process to produce carbon nanomaterials with unique chemical structures. Dynamic Light Scattering (DLS), micro-Raman and High-Resolution Transmission Electron Microscopy (HRTEM) were used to confirm the size distribution, morphology, chemical bonding, and crystallinity of these nanostructures. This article demonstrates how the fabrication process affects measured characteristics of the produced carbon nanomaterials. The obtained particle properties have potential use for various applications including biochemical speciation applications.

1. Introduction

Over the last two decades, there has been a growing interest in developing efficient methods for production of carbon nanoparticles (CNPs) due to their vast array of applications including polymeric nanocomposites, functional fillers, super-capacitors, and water purification [1]. Pulsed laser ablation (PLA) is one of the well-known methods used to produce CNP [2]. This method has been widely studied within vacuum and controlled atmosphere. In the late nineties, the laser ablation of samples submerged within liquid media was utilised for colloidal nanoparticle suspension preparation. This process became known as the Liquid Phase – Pulsed Laser Ablation (LP-PLA). LP-PLA provides control over particle size and morphology, material allotropes, and functionalisation where organic solvents are used as liquid media. This approach does not produce any byproducts, is of low cost and is considered easier to implement compared to the more conventional use of controlled vacuum or gaseous media environments [3].

During the LP-PLA process, ablation plumes are produced at the laser–target interaction site, where the target surface and the surrounding liquid are vaporised forming micro-bubbles. The bubbles expand to reach a certain critical combination of pressure and temperature and then collapse [4,5]. Within the bubbles, the temperature reaches thousands of Kelvin and pressures in the range of kPa to several GPa are achieved, producing novel materials [3]. In previous works, LP-PLA was undertaken using a low pulse repetition frequency (PRF), typically in the

range from 10 Hz to 30 Hz. In this study, the effect of using a Nd:YAG laser with a higher PRF in the range from 10 kHz to 14 kHz, and correspondingly an increased accumulated laser fluence (F) range, was investigated.

2. Materials and methods

Five millimetre diameter graphite rods of 300 mm length, MCCA medium grade, were obtained from Olmec Advanced Materials Ltd. The rods were cut to provide 6 mm lengths. A procedure for sample set-up before processing was composed of controlled steps to avoid possible contamination of the graphite rods. These steps were sample cleaning with deionised water, placement of the sample within the well plate reservoir which was 11 mm in height, filling of the well with deionised water, placement of a cleaned 200 m thick slide of soda lime glass on top of the well plate, and then positioning of the sample onto the laser ablation stage mount. This left a 5 mm gap between the graphite rod surface and the glass surface. Then, an area of 3 mm × 3 mm was ablated from the graphite target using a WEDGE HF 1064 nm wavelength and 700 ps pulse width Nd:YAG laser.

Typically, breakdown of the carbon material with pulses of 700 ps will occur via avalanche ionisation. For pulse durations longer than a few tens of picoseconds, energy is transferred from the laser-excited electrons to the lattice on the time scale of the pulse duration. Avalanche ionisation is therefore very efficient for pulses longer than a few picoseconds because the long pulse duration allows more time for exponential growth of the electron density. This energy is carried out of the focal volume by thermal diffusion. Damage then occurs when the temperature of the material in the irradiated region becomes high enough for the material to melt or fracture. The electron temperature increases within a few tens of femtoseconds and the laser energy is transferred from electron-to-lattice typically on the order of 10 ps. After this and within the laser-supported combustion range of laser intensities, a plasma is formed above the workpiece which starts to shield the incident power from the material surface [6]. As this plasma expands radially, energy within the plasma is coupled to the surface. The calculation of exact energy quality transfer to the surface is therefore convoluted by these effects. Higher fluences however still be expected to lead to increased initial electron temperatures, higher energy diffusion through the workpiece, better coupling from plasma to the workpiece surface, and ultimately to higher energy transmission to the target.

The number of pulses (N), PRF, and F were varied to investigate their effects on the carbon nanostructures produced. These parameters were adjusted according to a Box-Behnken experimental design (with 15 points in the experimental design space including three repetitions of the central point). The number of pulses was set to 1200, 1500 and 1800; frequency was set to 10, 12, and 14 kHz; and laser fluence was set to 0.3, 0.6, and 0.9J/cm^2. The laser fluence was kept below 1J/cm^2 as this was the maximum energy density available from the laser system at 14kHz. Fluences below 0.3J/cm^2 produced some ablation but did not produce any detectable levels of carbon nanoparticles. Laser ablation of the graphite rod surface produced a fine colloidal suspension within the deionised water consisting of carbon nanostructures. From each experiment, this colloid was pipetted into 1.5 mL Eppendorf centrifuge tubes using a glass pipette for subsequent characterisation. The colloids were

sonicated for 10 min, and then filtered using 200 nm syringe filters. The carbon nanoparticles were characterised for size distribution and appearance with a ZS90 Zetasizer (Malvern Instruments) and an FEI Tecnai F20, high resolution transmission electron microscope (HR-TEM). Chemical composition was analysed using a Jobin-Yvon Horiba LabRam® HR800 micro-Raman system at 20mW and $1\mu m^2$ spot size (with Ar^+ 488nm air cooled laser). Ten separate samples were prepared and average results calculated for the presented Zetasizer results.

3. Results and discussion

3.1 Particle size analysis

The average size and associated distribution differed depending on the laser processing parameters. Two distributions of nanostructure sizes were detected from all of the produced samples. Thus, all samples were separated into two different fractions by filtration, one fraction containing particles with sizes below 200 nm and the other with sizes above 200 nm. The z-average hydrodynamic size (intensity average by cumulants analysis), of sample fractions with particle sizes below 200 nm, is presented in Fig. 1. The figure shows the effects of N, PRF, and F on the size of the particles obtained. These 3D graphs were generated, in Design Expert®, using an absolute error reducing linear model.
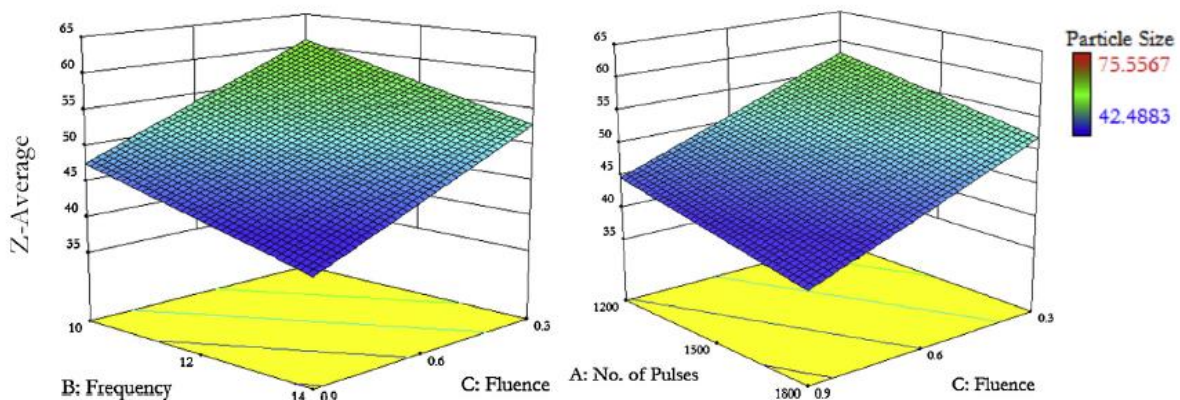

Fig. 1. Effects of number of pulses (N), PRF, and fluence (F) on fabricated particle sizes.

Measured data and fitted surface matched within 1%. The determined particle sizes were found to range from 42 to 75 nm (PDI values ranged from 0.15 to 0.26). These figures show that an increase in N, PRF, and F resulted in smaller z-average values. Smaller average particle sizes of 15 nm have been noted from use of 7 ns pulse width frequency doubled 532 nm Nd:YAG which may be attributable to enhanced absorbance at lower wavelengths [7].

3.2 Raman spectroscopy

The Raman spectra of the as received graphite and one of the filtered colloidal samples (particle size below 200 nm) are shown in Fig. 2.
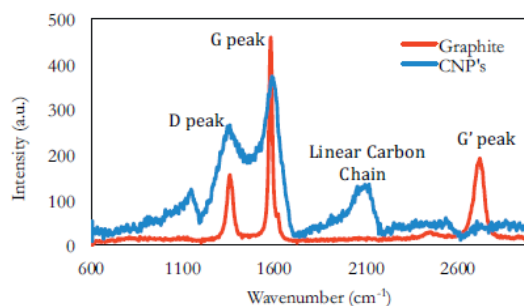
Fig. 2. Micro-Raman spectra for sample CNPs produced with 1500 pulses, 10 kHz, 0.9 J/cm² , and pure graphite.

The D, G, and G peaks for the as received graphite sample were at 1350, 1580, and 2700cm^{-1}, respectively. These fall well within the expected bands for carbon materials for visible excitation [8–12]. The ratio of the intensities of the D and G band [I_D/I_G] is used as a measure of disorder in graphitic materials. For the as received graphite and the unfiltered laser processed samples this was approximately 0.30 and 0.64, respectively. All of the laser processed materials produced D and G peaks at similar wavelengths in the Raman spectra as commonly observed and expected for carbon materials from the coexisting sp3 and sp2 phases. Higher ratios were determined for the laser produced carbon nanoparticles (in the range of 0.90–0.99) than for the as received graphite, indicating that they contained a less ordered crystalline phase compared to the commercial graphite material. The relative intensities of the D band further implies that carbon nanoparticles are highly defective which was also in accordance with the HRTEM and XPS data (not shown), although the nature of the defects associated with the graphite D band is a matter of debate. The G band was broad for the CNP colloidal samples, which suggests the presence of an imperfect carbon shell around the particles [13]. The G peak position for the laser processed CNPs was also shifted to higher wavelengths than that normally expected for the graphitic carbon, indicating the occurrence of some transformation of ordered graphite to nanocrystalline graphite [14]. The additional strong peak around 2100cm^{-1} represents linear carbon chain [15].

3.3 TEM

From TEM results the sample fractions with particle sizes below 200 nm were found to consist of nanocrystalline CNPs, whereas the sample fractions with particle sizes above 200 nm were found to additionally contain multi-walled carbon nanotubes (MWCNTs). Different sizes were visible from the TEM images, which corresponded with the trends observed from the Dynamic Light Scattering particle size analysis measurements. From HRTEM results it was found that the laser fluence was the main parameter that affected the type of carbon nanostructure produced.
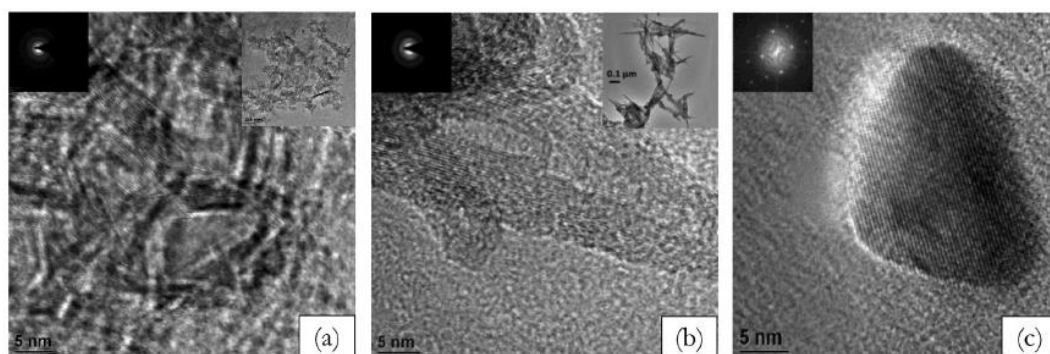
Fig. 3. (a) HRTEM image of OLCs synthesized using 1500 pulses, 14 kHz, and 0.3 J/cm². (b) HRTEM image of MWCNPs synthesized at 1500 pulses, 12 kHz, and 0.6 J/cm², and (c) HRTEM image of a CNP synthesized at 1200 pulses, 12 kHz and 0.9 J/cm². The left hand side insets in (a) and (b) show SAED, and in (c) the FFT for the HRTEM images.

At $0.3 J/cm^2$ Onion Like Carbons (OLCs) were synthesised, as shown in Fig. 3(a). The existence of sharp diffraction rings in the Selected Area Electron Diffraction (SAED) pattern (inset in Fig. 3(a)) indicates the characteristic amorphous structure of the OLCs [13,16,17] Fig. 3(b) represents the unfiltered sample at a laser fluence of $0.6 J/cm^2$ at which MWCNTs were synthesised. A larger number of MWCNTs can be seen in the right hand inset of Fig. 3(b), while the left side inset shows that the diffraction pattern of this MWCNT sample revealed prominent graphitic (0 0 2) and (0 0 4) diffraction ring [18]. Fig. 3(c) shows the HRTEM image of a single CNP synthesised using $0.9 J/cm^2$ laser fluence. The corresponding d-space for the particle is 0.364 nm, signifying a graphitic carbon nanoparticle [14,19]. The left side inset represents the Fast Fourier Transform (FFT) of the CNPs indicating a single crystalline structure.

4. Conclusion

The higher frequency of processing used in this study permitted the use of increased energy density per unit time and per unit area. Due to the resulting high temperatures and pressures that this generated within the collapsing bubbles, novel material structures were formed. LP-PLA could be used to produce both crystalline CNPs and carbon nanotubes (CNTs). In this work, CNPs with a size distribution range below 200 nm and, CNPs and CNTs with a size distribution range above 200 nm were produced. The two fractions were separated by filtering and the lower size range CNPs were analysed in detail. The Z-average size of the nanoparticles in suspension was found to range between 42 and 75 nm. Increased N, PRF and F resulted in higher energy density and in the fabrication of nanoparticles with smaller sizes. With increased laser fluence, the temperature and pressure within the hot plasma increases which may contribute to further particle melting, fracturing, and smaller particle sizes [20]. The liquid-confined plasma pulse width is also 2–3 times longer than the applied laser pulse duration [21], which can amplify the plasma plume effect within the LP-PLA process compared to less dense atmospheres. The high degree of repeatability and narrow size distribution found for the carbon nanoparticles in this work suggests their possible use as materials for functional separation science applications. A wide variety of device types have been developed within which such CNPs could be incorporated [22,23] for biochemical applications [24].

Acknowledgements

References

[1] D. Pech, M. Brunet, H. Durou, P. Huang, V. Mochalin, Y. Gogotsi, P. Taberna,P. Simon, Ultrahigh-power micrometre-sized supercapacitors based on onion-like carbon, Nature Nanotechnology 5 (2010) 651–654.

[2] P.R. Willmott, J.R. Huber, Pulsed laser vaporization and deposition, Reviews ofModern Physics 72 (January (1)) (2000) 315–328.

[3] D. Amans, A.-C. Chenus, G. Ledoux, C. Dujardin, C. Reynaud, O. Sublemontier, K.Masenelli-Varlot, O. Guillois, Nanodiamond synthesis by pulsed laser ablationin liquid, Diamond and Related Materials 18 (2009) 177–180.

[4] O. Yavas, A. Schilling, J. Bischof, J. Boneberg, P. Leiderer, Bubble nucleation andpressure generation during laser cleaning of surfaces, Applied Physics A 64(1997) 331–339.

[5] L. Yang, P.W. May, L. Yinb, J.A. Smith, K.N. Rosser, Growth of diamond nanocrys-tals by pulsed laser ablation of graphite in liquid, Diamond and RelatedMaterials 16 (2007) 725–729.

[6] Y.-I. Lee, K. Song, J. Sneddon, Laser-Induced Breakdown Spectrometry, NovaScience Publishers Inc., 2000.

[7] G.X. Chen, M.H. Hong, L.S. Tan, T.C. Chong, H.I. Elim, W.Z. Chen, W. Ji, Opti-cal limiting phenomena of carbon nanoparticles prepared by laser ablation inliquids, Journal of Physics: Conference Series 59 (2007) 289–292.

[8] S.R.J. Pearce, S.J. Henley, F. Claeyssens, P.W. May, K.R. Hallam, J.A. Smith,K.N. Rosser, Production of nanocrystalline diamond by laser ablation at thesolid/liquid interface, Diamond and Related Materials 13 (2004) 661–665.

[9] Y. Zhang, Z. Shi, Z. Gu, S. Iijima, Structure modification of single-wall carbonnanotubes, Carbon 38 (2000) 2055–2059.

[10] A.C. Ferrari, J. Robertson, Raman spectroscopy of amorphous, nanostructured,diamond-like carbon, and nanodiamond, Philosophical Transactions of TheRoyal Society A 362 (2004) 2477–2512.

[11] S.Z. Mortazavi, P. Parvin, A. Reyhani, Fabrication of graphene based on Q-switched Nd:YAG laser ablation of graphite target in liquid nitrogen, LaserPhysics Letters 9 (7) (2012) 547–552.

[12] N.N. Melnik, P.N. Lebedev, Optical properties of carbon nanoparticles, in: J.A.Garrido, K. Haenen, D. Ho, K.P. Loh (Eds.), MRS Spring Meeting, vol. 1362, 2011,http://dx.doi.org/10.1557/opl.2011.1173.

[13] Fan Jung-Chuan, Sung Huang-Huei, Lin Chun-Rong, Lai Mei-Hsiu, The produc-tion of onion-like carbon nanoparticles by heating carbon in a liquid alcohol,Journal of Materials Chemistry 22 (19) (2012) 9794–9797.

[14] A. Rahy, C. Zhou, J. Zheng, S.Y. Park, J. Moon, I. Kim, S.J. Jang, D.J. Cho Yang,Photoluminescent carbon nanoparticles produced by confined combustion ofaromatic compounds, Carbon 50 (3) (2012) 1298–1302.

[15] L. Ravagnan, F. Siviero, C. Lenardi, P. Piseri, E. Barborini, P. Milani, C.S. Casari,A. Li Bassi, C.E. Bottani, Cluster-beam deposition and in situ characterization ofcarbyne-rich carbon films, Physical Review Letters 89 (28) (2002), pp. 285506-(1-4).

[16] M. Sh. Sharif, F. Golestani Fard, E. Khatibi, H. Sarpoolaky, Dispersion andstability of carbon black nanoparticles, studied by ultraviolet–visible spec-troscopy, Journal of the Taiwan Institute of Chemical Engineers 40 (5) (2009)524–527.

[17] S.-L. Hu, K.-Y. Niu, J. Sun, J. Yang, N.-Q. Zhao, X.-W. Du, One-step synthesisof fluorescent carbon nanoparticles by laser irradiation, Journal of MaterialsChemistry 19 (4) (2009) 484–488.

[18] B. Wen, J. Zhao, T. Li, C. Dong, J. Jin, n-diamond from catalysed carbon nano-tubes: synthesis and crystal structure, Journal of Physics: Condensed Matter 17(December (48)) (2005) L513–L519.

[19] L. Tian, Y. Song, X. Changa, S. Chen, Hydrothermally enhanced photo-luminescence of carbon nanoparticles, Scripta Materialia 62 (11) (2010)883–886.

[20] G. Bajaj, R.K. Soni, Effect of liquid medium on size and shape of nanopar-ticles prepared by pulsed laser ablation of tin, Applied Physics A 97 (2009)481–487.

[21] L. Berthe, R. Fabbro, P. Peyre, L. Tollier, E. Bartnicki, Shock waves from awater-confined laser-generated plasma, Journal of Applied Physics 82 (1997)2826.

[22] M. Vázquez, D. Brabazon, F. Shang, J.O. Omamogho, J.D. Glennon, B. Paull,Centrifugally-driven sample extraction, preconcentration and purification inmicrofluidic compact discs, TrAC – Trends in Analytical Chemistry 30 (10)(2011) 1575–2158.

[23] M. Ryvolová, M. Mirek, D. Brabazon, J. Preisler, Portable capillary-based (non-chip) capillary electrophoresis, TrAC – Trends in Analytical Chemistry 29 (4)(2010) 339–353.

[24] J.A. Ho, Y.C. Lin, L.S. Wang, K.C. Hwang, P.T. Chou, Carbon nanoparticle-enhanced immunoelectrochemical detection for protein tumor marker withcadmium sulfide biotracers, Analytical Chemistry 81 (4) (2009) 1340–1346.